

Nanorobotic Mass Transport

Zheng Fan¹, Xinyong Tao², Xiaobin Zhang³ and Lixin Dong^{1,*}

¹Department of Electrical and Computer Engineering, Michigan State University, East Lansing, MI 48824-1226, USA

²College of Chemical Engineering and Materials Science, Zhejiang University of Technology, Hangzhou 310014, China

³Department of Materials Science and Engineering, Zhejiang University, Hangzhou 310027, China

Email: fanzheng@egr.msu.edu, xinyongtao@gmail.com, zhangxb@zju.edu.cn, ldong@egr.msu.edu

Abstract — Mass transport at attogram (10^{-18} g) level inside, from, between, and into nanochannels is of growing interest from both fundamental and application perspectives. Nanorobotic manipulation inside a transmission electron microscope (TEM) enables these investigations through its ability to position and assemble pipes, to deliver the mass in a controlled way, and to tune and characterize these systems *in situ*. Mass transport systems at this scale provide a platform for the investigation of nanofluidics and can serve as components for nanomanufacturing such as electromigration-based deposition (EMBD) for prototyping nanostructures. In such applications, the limited mass initially encapsulated inside a nanotube will obviously become a bottle neck. Continuous mass feeding, which involves the mass flow into a nanotube from a reservoir, is proposed as a solution. This technique enabled a new path for the design of an EMBD system. As a general-purposed nanofabrication process, EMBD will enable a variety of applications such as nanorobotic arc welding and assembly, nanoelectrodes direct writing, and nanoscale metallurgy.

Index Terms – mass transport, electromigration, nanorobotic manipulation, continuous feeding, nanostructure

I. INTRODUCTION

Mass transport at attogram (10^{-18} g) level inside, from, between, and into nanochannels (Figure. 1) is of growing interest from both fundamental and application perspectives [1-3]. Carbon nanotubes (CNTs), with their extremely strong mechanical strength and nanometer-sized hollow cores, are ideal candidates for nanochannels. Nanorobotics enables these nanometer-scale systems through its ability to position and assemble pipes, to deliver the mass in a controlled way, and to tune and characterize these systems *in situ*. Mass transport systems at this scale provide a platform for the investigation of nanofluidics based nano-device and can serve as components for nanomanufacturing such as nanotube fountain pen (NFP) for prototyping nanostructures [4].

CNT-based mass transport began with a demonstration of the axial thermal expansion of gallium inside a CNT. The expansion of the gallium inside a nanotube was used as a thermometer [1] to indicate the surrounding temperature. Gallium's macroscopic expansion properties are retained at the nanometer scale. By associating the end-to-end nanotube resistance with the temperature, a sensor with a readout device independent to the microscopy images was invented [5]. The resistance of the Ga-filled nanotube changes when the gallium expands. Recently, a nanoshuttle memory device [6] was proposed, where Au iron nanoparticle shuttle is controllably positioned within a hollow nanotube channel

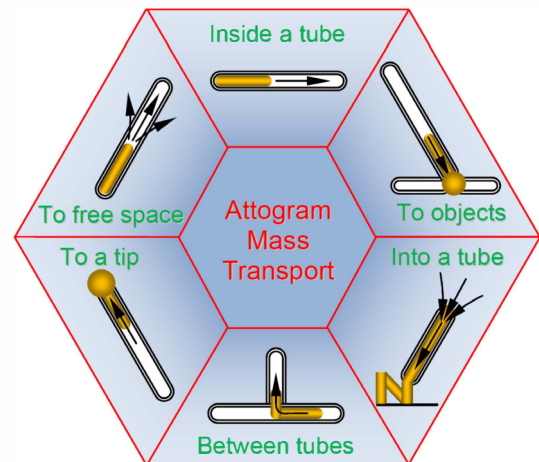


Fig. 1 Nanorobotic mass transport inside, from, between, and into nanotubes.

based on electromigration. Different positions of the nanoparticles are used to represent information. The information density can be as high as 10^{12} bits/in², and thermodynamic stability is excess of one billion years. Because of the fluidic pressure on the side walls of a CNT, metal flowing inside a bent CNT can induce deformation. This flow-induced deformation can find potential applications as a switch or an actuator. Nanofluidic junctions [7] and networks [8] involve the mass transport between nanotubes.

II. MASS TRANSPORT USING NANOTUBES

The mass transport between, into and out from nanotubes are significant for forming a fluidic system. Flowing out from a nanotube can generate a variety of results based on the targets (Figure 1). Evaporation to a free space is a result of discharging, ionization, or heating.

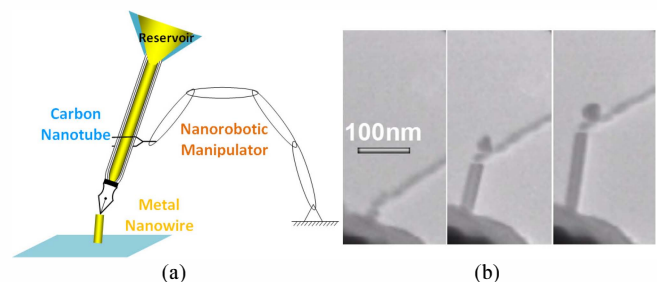


Fig. 2 (a) The NFP technique is prototyped using a metal-filled carbon nanotube (m-CNT) as a pen-tip injector and a network of m-CNTs as a reservoir for continuous mass feeding. (b) Controlled mass feeding.

Deposition on a surface can be obtained if placing the nanotube tip against such a target. Nanorobotic spot welding [9] is based on mass transport to the interface between two objects. As an emerging additive nanolithography technique, “writing” with a nanotube fountain pen (NFP) is a more general technique representing the mass transport of metallic materials against a surface (Fig. 2(a)). Free-standing nanostructure can be formed on the tip of the injector nanotube if moving it back from the target (Fig. 2(b)) [10]. Likewise, the mass transportation between the tubes potentializes the mass refill of the nanotube-injector, producing a “reloading” procedure.

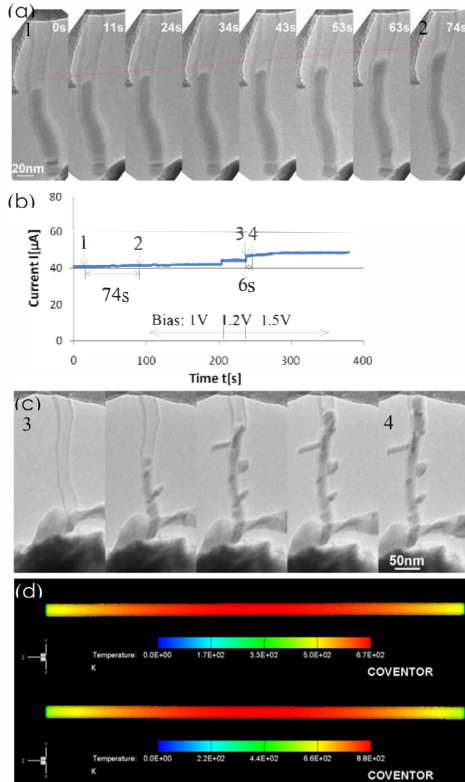


Fig. 3 (a) The reloading in a Cu@CNT with a lower inputted energy, the process lasts for 74 s. (b) Current-time characterization about reload process with different inputted energy. (c) The reloading process with higher electrical energy, the reload process lasts for 6 s. (d) The simulation of the thermal distribution along a CNT as the external bias increased.

Nanorobotic mass transport based NFP “writing” can be realized under a low bias (typically several volts). In previous investigations, the electromigration effect has been confirmed as the main possible mechanism for the flow. Moreover, the studies in “reloading” reveals that the electromigration effect is also responsible for the mass transport between nanotubes, which made it possible to feed mass from neighbor tubes to the injector. As shown in Fig. 3(a), the “reloading” process (frames 1-2) occurs as the external bias reaches 1 V; whereas, due to the lower input driven energy, only a few amount of mass has been melted and transported, and the mass accumulation speed during 74 s is only 0.52 nm/s (Fig. 3(b)). In contrast, as we increased the bias voltage up to 1.5 V, a huge mass reloading suddenly occurred (Fig. 3(c)). During this process (frames 3-4, 6 s),

the mass transport speed reaches up to 96.2 nm/s. We simulate the NFP under these two external voltages to understand the nature of mass reloading. The NFP has been simulated as a single cylinder nanostructure (Fig. 3(d)), and the current induced thermal distribution illustrate that the high temperature portion along the tube (red portion) would enlarge due to the increase of the bias from 1.0 V to 1.5 V. This allows more mass to get melt, and with the increase of the electromigration force, the transport of these mass is readily to be realized. Therefore, it can be concluded that, the increased input of electric energy induces the mass melting and migration in a large amount, which provides potential to reloading the mass.

III. MECHANISM

The question remaining is the effect driven the mass migration. In previous investigations, several hypotheses have been taken to elucidate the fundamental mechanism of the mass migration between, into and out from tubes [2, 9, 11-14]. Here we engineer the NFP to *in situ* investigate the nature of mass transport. We start the experiment from a Cu@CNT without a mass reservoir (Fig. 4(a)). By applying a bias voltage on this tube, the anode is on the lower side and the cathode is on the upper side. When the external bias reached 2.0 V (0 s), the dark contrast and the boiling sign indicate the molten state of the copper wire. As the bias is increased into 2.2 V (7 s), the inner mass was suddenly separated in the center, migrating to the two ends and formed a “gap” in the center. Nevertheless, by further adding the voltage in steps of 0.1 V intervals until the external bias reached 2.5 V (11s), it can be noted that the mass began to transport in the unique direction from upper part to the lower part. As we conduct the same experiment on a nanotube installed with a reservoir, the process is similar to the previous one; initially, the inner mass split and finally flowed in the same direction, as the reservoir enables considerable volume capacities; the mass from the reservoir continuously injected into the nanotube and finally fulfilled the gap. In Fig. 4(b), the relation between the transferred mass and time inside the tube was given as: $m = 0.0168t^2 - 0.0681t + 1.9971$. Thus, the flow rate was expressed as: $dm/dt = 0.0336t - 0.0681$, indicating a linear mass flow rate to the time. From these two experiments, we conclude that, there are at least two sessions during the mass transport, which implies that there might be more than a single effect existing during the mass migration.

On the basis of the experimental results, we proposed a general model (Fig. 4(c)) to elucidate the effects during the mass flow. At the beginning of the mass split process, the current is in low profiles. Thus the migration is ceased, which in turn produces a lower electromigration force. If we assume the mass migration is driven by this effect, the mass in Figs. 4(a) and (b) should consistently move towards cathode to anode. In contrary, the mass move from center towards the two ends. According to the center of the nanotube was presumed to be the high-resistance point or

“hottest spot” [15-17], parts of the mass was evaporated and the thermal gradient in turn diverted from the center towards the cooler locales (the two ends of tube), which highly suggestive of a thermal gradient effect at the beginning to evaporate the mass and driven the flow. However, as the current is sharply increased, the electromigration force was reinforced and dominant the main role for the migration, which results the mass ultimately flows from cathode to anode consistently.

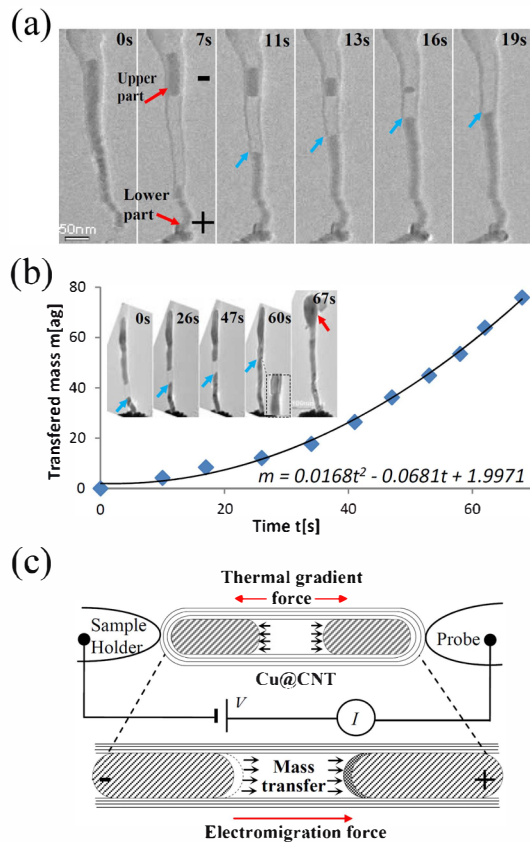


Fig. 4 The mechanism analysis of NFP “writing”. (a) The process shows the competition between electromigration force and thermal gradient force during the mass transportation process. When the bias reached 2.2 V, the inner mass was separated in the center and transferred to the two ends, formed a “gap”. As the center of the nanotube was presumed to be the high-resistance point, or “hottest spot,” the thermal gradient force in turn diverted from the center towards the two ends; therefore, the inner mass split process is obviously attributed to the actuation of temperature gradient force. By further adding the voltage at 0.1 V intervals until the external bias reached 2.5 V, it can be noted that with the reinforcement of electromigration effect, the mass is transferred from the upper part to the lower part in an average rate of 2.2 ag/s. (b) The mass flow rate study on a Cu@CNT combined with a network reservoir. The relation between the transferred mass and time inside the tube was given as: $m = 0.0168t^2 - 0.0681t + 1.9971$. Thus, the flow rate was expressed as: $dm/dt = 0.0336t - 0.0681$, indicate a linearly accessed mass flow. (c) The modeling of the mass transport.

The NFP mass flow rate also shows a linearly correspondence to the applied current after the mass starts to migrate. When the driven bias was increased by intervals of 0.2 V (Fig. 5(a)), the current curve shows a remarkable regular staircase with step sizes of about 1.2 μ A, and the mass flow rate was also accelerated. The relation between the mass flow rate and the current value suggests a linear

ratio: $M = 5.53I^2 - 257.19I + 2994.0$. Likewise, the representative images in Fig. 5(a), inset demonstrate that the diameter of a deposited nanowire (17 nm) is comparable to the tube (18 nm). Actually, all the nanowires we have achieved yield the similar size to the original tube. It is therefore assumed that, the diameter of delivered metal nanowires is comparable to the size of the encapsulated nanotubes. The beginning of the mass feeding process can be simulated as follows (Fig. 5(b)): As the external driven voltage/current is large enough, the copper atom would pass through the junction and form the conductive filament channel between the inner copper and the probe surface. Then, the resistivity of the neighbor holes would largely decreased, the copper flowing out and generating a nanowire with similar size to the tube. It is crucial to note that the electric energy (applied voltage and current) required to break down the junction is largely related to the size of tube. The simulations are undergoing for fully understanding, as illustrated in Fig. 5(c), we modeled the nanotube injector and network combined NFP system as single Cu@CNTs in diameters of 12 and 20 nm respectively. With a bias (2V) added on the two ends of them, the current distributions along the tube can be plotted, as well as thermal distributions. According to the intensified current density in the small tube, the temperature profile along the nanotube with a small diameter is apparently higher than with the larger one. Additionally, the intensified current would induce greater electromigration force, this helps the copper atom pass the energy barrier and collapse the blocked junction between the tube and the deposited surface. However, to the CNTs with a large size, higher power will be needed. Table I suggests that the injected electrical power P ($P=IV$) for the tubes in different sizes to realize the mass flow out. The diameter-power (DP) curve is fitted by: $D = 0.0532P + 27.508$ (Fig. 5(d)), which suggests the linear increasing of P to the larger nanotube.

As the nanowires were written on the object, the shape of them was formed immediately due to the excellent thermal conductivity of the probe that cools down the deposit.^[18] Reheating of the cooled-down deposit was hardly achieved because the volume of the probe (tip radius: 120 nm, root radius: 10 μ m) is absolutely larger than that of the copper deposit. The probe serves as a heat sink with essentially infinite capacity compared with the copper deposit. A detail examination of the crystalline structure of the generated nanowire can further understand the shaping process of it. Fig. 5(e) illustrates the crystalline analysis of the generated nanowire. At the contact area between the probe and nanotube (area I), the crystalline of deposited copper shows a poly-crystal phase, rather than a single-crystalline. This is attributed to the instant cool down from the heat sink; the molten mass has not crystallized enough before it formed the solid state. In contrast, the phase in area II reveals a single-crystalline since it is far from the heat sink. Moreover, according to the dark contrast and the amorphous phase illustrated at area III, we can confirm the molten state at this position. Therefore, the molten state at area III

provides possible to shaping the deposit by manually position the injector to shape the final feature of the structure.

the ‘Qianjiang Scholars’ program and the project sponsored by SRF for ROCS (2010609), SEM.

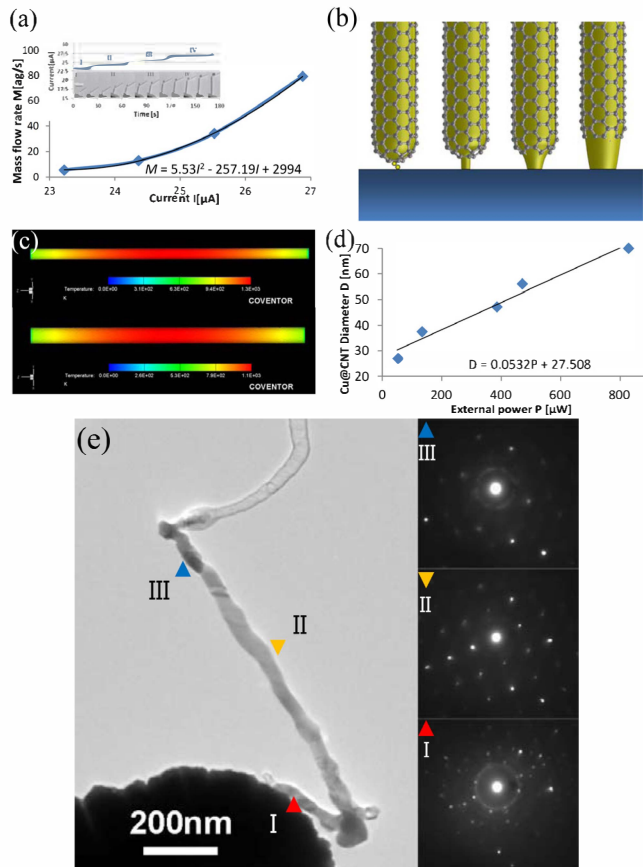


Figure. 5 The process analysis of NFP “writing”. (a) During the “writing”, the mass flow rate changes along the acceleration current. Insets show the representative TEM images at different acceleration current and the current curve shows a remarkable regular staircase with step sizes of about 1.2 μA as the driven bias increased on the step of 0.2 V. The size of the generated nanowire is comparable to the diameter of tube. (b) The simulation of the mass flowing out process. (c) The simulation of the thermal distribution along different sized NFP. It shows that the nanotube with small diameter has higher temperature than the one with large diameter. (d) Correlation of the NFP diameter D with the external electric energy. (e) The crystalline phase analysis of as-generated nanowire. Due to the molten state at the connection between the deposit and the injector, it provides possible to shape the deposited structure.

IV. SUMMARY

In summary, we have experimentally investigated different forms of the mass transport in a nanofluidic system using nanorobotic manipulation inside a TEM. Based on the “reloading” and “writing” processes, the nature of the transport has been analyzed. Nanorobotic mass transport will enable a variety of applications such as nanotube plumbing system, nanorobotic arc welding, and nanoscale metallurgy.

ACKNOWLEDGMENT

This work is supported by the NSF (IIS-1054585), the NSFC (51002138), the Zhejiang Provincial NSF of China (Y4090420), the Qianjiang Talent Project (2010R10029),

REFERENCES

- [1] Y. H. Gao and Y. Bando, "Carbon nanothermometer containing gallium - Gallium's macroscopic properties are retained on a miniature scale in this nanodevice," *Nature*, vol. 415, no. 6872, pp. 599, Feb 2002.
- [2] K. Svensson, H. Olin, and E. Olsson, "Nanopipettes for metal transport," *Physical Review Letters*, vol. 93, no. 14, art. no. 145901, Oct 2004.
- [3] L. Sun, F. Banhart, A. V. Krasheninnikov, J. A. Rodriguez-Manzo, M. Terrones, and P. M. Ajayan, "Carbon nanotubes as high-pressure cylinders and nanoextruders," *Science*, vol. 312, no. 5777, pp. 1199-1202, May 2006.
- [4] Z. Fan, X. Y. Tao, X. B. Zhang, and L. X. Dong, "Towards nanotube fountain pen," in *Nanotechnology (IEEE-NANO), 2011 11th IEEE Conference*, Portland, 15-18 Aug. 2011, pp. 596-599.
- [5] P. S. Dorozhkin, S. V. Tovstonog, D. Golberg, J. H. Zhan, Y. Ishikawa, M. Shiozawa, H. Nakanishi, K. Nakata, and Y. Bando, "A liquid-Ga-fitted carbon nanotube: A miniaturized temperature sensor and electrical switch," *Small*, vol. 1, no. 11, pp. 1088-1093, Nov 2005.
- [6] G. E. Begtrup, W. Gannett, T. D. Yuzvinsky, V. H. Crespi, and A. Zettl, "Nanoscale Reversible Mass Transport for Archival Memory," *Nano Letters*, vol. 9, no. 5, pp. 1835-1838, May 2009.
- [7] X. Y. Tao, L. X. Dong, W. K. Zhang, X. B. Zhang, J. P. Chen, H. Huang, and Y. P. Gan, "Controllable melting and flow of Beta-Sn in flexible amorphous carbon nanotubes," *Carbon*, vol. 47, no. 13, pp. 3122-3127, Nov 2009.
- [8] L. X. Dong, X. Y. Tao, L. Zhang, X. Zhang, and B. Nelson, "Plumbing the depths of the nanometer scale," *Nanotechnology Magazine, IEEE*, vol. 4, no. 1, pp. 13-22, Mar 2010.
- [9] L. X. Dong, X. Y. Tao, L. Zhang, X. B. Zhang, and B. J. Nelson, "Nanorobotic spot welding: Controlled metal deposition with attogram precision from copper-filled carbon nanotubes," *Nano Letters*, vol. 7, no. 1, pp. 58-63, Jan 2007.
- [10] Z. Fan, X. Y. Tao, X. D. Cui, X. D. Fan, and L. X. Dong, "Spheres on pillars: Nanobubbling based on attogram mass delivery from metal-filled nanotubes," in *Nanotechnology (IEEE-NANO), 2010 10th IEEE Conf*, Seoul, Korea, 17-20 Aug. 2010, pp. 649-654.
- [11] S. Heinze, N. P. Wang, and J. Tersoff, "Electromigration forces on ions in carbon nanotubes," *Physical Review Letters*, vol. 95, no. 18, art. no. 186802, Oct 2005.
- [12] B. C. Regan, S. Aloni, R. O. Ritchie, U. Dahmen, and A. Zettl, "Carbon nanotubes as nanoscale mass conveyors," *Nature*, vol. 428, no. 6986, pp. 924-927, Apr 2004.
- [13] A. Barreiro, R. Rurali, E. R. Hernandez, J. Moser, T. Pichler, L. Forro, and A. Bachtold, "Subnanometer motion of cargoes driven by thermal gradients along carbon nanotubes," *Science*, vol. 320, no. 5877, pp. 775-778, May 2008.
- [14] J. O. Zhao, J. Q. Huang, F. Wei, and J. Zhu, "Mass Transportation Mechanism in Electric-Biased Carbon Nanotubes," *Nano Letters*, vol. 10, no. 11, pp. 4309-4315, Mar 2010.
- [15] P. G. Collins, M. Hersam, M. Arnold, R. Martel, and P. Avouris, "Current saturation and electrical breakdown in multiwalled carbon nanotubes," *Physical Review Letters*, vol. 86, no. 14, pp. 3128-3131, Apr 2001.
- [16] J. Y. Huang, S. Chen, S. H. Jo, Z. Wang, D. X. Han, G. Chen, M. S. Dresselhaus, and Z. F. Ren, "Atomic-scale imaging of wall-by-wall breakdown and concurrent transport measurements in multiwall carbon nanotubes," *Physical Review Letters*, vol. 94, no. 23, art. no. 236802, Jun 2005.
- [17] X. Y. Huang, Z. Y. Zhang, Y. Liu, and L. M. Peng, "Analytical analysis of heat conduction in a suspended one-dimensional object," *Applied Physics Letters*, vol. 95, no. 14, art. no. 143109, Oct 2009.
- [18] Z. Fan, X. Y. Tao, X. D. Cui, X. D. Fan, X. B. Zhang, and L. X. Dong, "Shaping the nanostructures from electromigration-based deposition," in *Proc. of the 2010 IEEE Nanotechnology Materials and Devices Conference (IEEE-NMDC2010)*, Monterey, California, Oct. 12-15, pp. 22-25.